Physical Modeling of GaAs MESFET's in an Integrated CAD Environment: From Device Technology to Microwave Circuit Performance

GIOVANNI GHIONE, MEMBER, IEEE, CARLO U. NALDI, MEMBER, IEEE, AND FABIO FILICORI

Abstract—**A CAD environment leading from technology to performance evaluation by integrating process, device, and circuit simulation would be a valuable tool for the development of monolithic microwave circuits. The paper focuses on the linkage between a physical device simulator for small- and large-signal characterization, and CAD tools for both linear and nonlinear circuit analysis and design. Efficient techniques are presented for the physical dc and small-signal analysis of MESFET's; then, the problem of physical simulation in a circuit environment is discussed, and it is shown how such a simulation makes it possible to obtain small-signal models accounting for propagation and external parasitics. Finally, efficient solutions are proposed for physical large-signal simulation, based on deriving large-signal equivalent circuits from small-signal analyses under different bias conditions. The small- and large-signal characterizations thereby obtained allow physical simulation to be performed efficiently in a circuit environment. Examples and results are presented throughout the paper.**

I. INTRODUCTION

AN INTEGRATED CAD environment assisting the development of MMIC's (monolithic microwave integrated circuits) from the technological stage to the functional block level would be a very attractive and promising design tool. The need of a common CAD environment, integrating *process simulation*, *device simulation*, and *circuit analysis and design* naturally arises from the strong correlation existing in MMIC's between *device* and *circuit* design [41], [22], [7]. While GaAs process simulation is still comparatively underdeveloped, device simulation based on *physical models* is of growing importance in the field of GaAs device development as an instrument intrinsically able to provide correct feedback between technology and device behavior. As far as circuit analysis and design are concerned, the importance of CAD tools hardly needs to be stressed.

Manuscript received April 29, 1987; revised July 12, 1988. This work was supported in part by TELETTRA S.p.A and by the European Community through ESPRIT Project 255.

G. Ghione is with the Dipartimento di Elettronica, Politecnico di Milano, Piazza Leonardo da Vinci 32, Milan, Italy.

C. Naldi is with the Dipartimento di Elettronica, Politecnico di Torino, Corso Duca Abruzzi 24, Torino, Italy.

F. Filicori is with the Dipartimento di Elettronica Informatica e Sistemistica, Universitá di Bologna, Viale Risorgimento, 2, Bologna, Italy.

IEEE Log Number 8825381.

While interfacing *process* and *device* simulation is comparatively straightforward, problems arise when physical *device* simulation has to be linked with *circuit* simulation. It is not surprising that, although physical microwave device simulation has now reached maturity both in defining models and in devising techniques for their numerical solution, such models have up to now been mainly oriented to the technologist [16], and are poorly linked to CAD tools allowing the prediction of device performance in a realistic microwave circuit environment. Indeed, the linkage between *physical models* and *circuit simulation* does require the solution of certain basic problems which arise when physical models have to simulate *microwave* and *large-signal* device performances.

Since physical simulation can yield both the static and the time-domain response of the device under arbitrary excitation, *small-signal* and *large-signal* simulations are seemingly feasible directly in the time domain. Unfortunately, this simple and straightforward approach turns out to be unsatisfactory for a number of reasons:

- Two-dimensional physical simulation only accounts for the limited region of the device which is actually simulated, and neglects all external phenomena and parasitics (propagation along the gate, launchers, stray lead inductances, effect of package—if any, etc.) which assume greater importance at microwave frequencies. Direct inclusion in the physical simulator of such effects, modeled directly or as circuit elements, although theoretically possible, is extremely cumbersome in practice.
- While the *small-signal* characterization of the device can be performed in isolation, i.e., by driving the physical model with ideal sources, *large-signal* simulation must account for the presence of an external network connected to the device. *Direct* coupling between the large-signal time-domain physical model and the external network has actually been successfully performed in simple cases [43]. Unfortunately, this solution is extremely CPU intensive; in fact, while the almost intrinsic (simulated) device reaches

0018-9480/89/0300-0457$01.00

steady state in a few picoseconds, when such a device is coupled to an external network the expensive large-signal device simulation has to last as long as the slow time constants of the network require.

- Direct inclusion of a large-signal time-domain physical model into a full circuit analysis CAD environment is a formidable task; moreover, this strategy would be very difficult to apply to the powerful software tools already existing both for linear (e.g. SUPERCOMPACT, TOUCHSTONE, ACCAD [4]) and nonlinear (e.g. SPICE, QSS [32]) microwave circuit analysis.

The approach we propose to overcome these problems, so as to achieve an effective linkage between physical device simulation and circuit simulation, is based on classical measurement-oriented procedures which already allow the designer to pass from actual measurements to circuit-oriented device characterizations. Such a strategy has many advantages when compared to direct integration between time-domain device and circuit models:

- No large-signal time-domain analysis of the physical model is actually needed in order to derive a large-signal circuit model, which can be based on *small-signal* simulations under several bias conditions.
- Once an efficient small- or large-signal circuit-oriented model is available, external parasitic effects can easily be added as circuit elements.

However, it is also worth noting that physical modeling permits circuit-oriented models to be identified which are potentially superior to those derived from actual measurements. In fact, physical simulation allows the internal behavior of the device to be completely known, thereby leading to both better understanding of device operation and easier and more accurate identification of equivalent circuits.

The identification of large-signal models requires extensive device simulations to be performed in the $V-I$ plane, so as to obtain small-signal characterizations under several different bias conditions. In order to reach this goal with acceptable computer times, an accurate but handy physical model should be used, and its numerical implementation should try to optimize execution speed. A brief description of some new solutions adopted in the physical MESFET simulator MESS [18], [17], developed entirely by the authors within the framework of this research, is therefore in order. MESS, starting from technological inputs, can perform the steady-state, small-signal, and large-signal characterization in reasonable computer times (typically 4–6 CPU hours on a VAX780). By means of the small-signal and large-signal models resulting from simulation, complete feedback is obtained, at a comparatively low cost, between circuit performance and technology, according to the flow diagram outlined in Fig. 1.

The paper is structured as follows. First, the choice of a physical model is discussed, and efficient techniques are described for steady-state and small-signal simulation. Second, possible ways of deriving efficient small-signal and large-signal circuit-oriented characterizations from physical simulation are considered. Finally, microwave performance prediction through proper interfacing of the physical simulator with linear and nonlinear circuit analysis tools is discussed. Examples of steady-state and small-signal device simulation are presented throughout the paper.

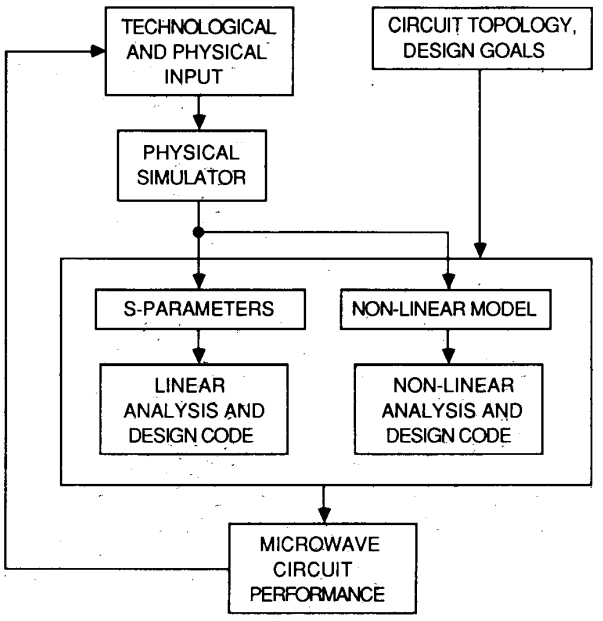

Fig. 1. Flow diagram of an integrated CAD tool for the simulation of MESFET devices from the technological stage to circuit performance evaluation.

II. The Physical Device Simulator

A. The Physical Model

Since physical models of widely different complexity exist (Boltzmann equation [27], energy transport models [5], [9], [11], [42], drift-diffusion models [40]) a compromise is needed between the completeness and accuracy of the model, and its computational efficiency. Single-gas energy transport models [42], which are currently being investigated, are still rather inefficient from a computational point of view when compared to the majority carrier drift-diffusion model. Although this model is inaccurate for very short devices, good agreement with experimental data for 0.5 μm MESFET's has been reported in the literature (see e.g. [43, fig. 6]) and confirmed by this research. This suggests that in the 1.0–0.5 μm range the drift-diffusion model, which has been adopted in MESS, can still be used as a basis for performance evaluation, perhaps in connection with heuristics aimed at accounting for nonstationary transport phenomena in an averaged way (e.g. through modified velocity-field curves [13] or high-field relaxation time expressions for diffusivity [45, eq. 10]). Moreover, one should not forget that phenomena such as surface effects, buffer traps [2], [25], and external circuit parasitics probably have a greater influence than

velocity overshoot on the overall behavior of devices operating up to (approximately) the K_u frequency band.

The model equations read

$$\frac{\partial n}{\partial t} - \nabla \cdot [n\mu(E)\boldsymbol{E} + D(E)\nabla n] + R = 0 \tag{1}$$

$$\nabla^2 \phi = -\alpha(N_D - n), \qquad \alpha = q/\epsilon_0 \epsilon_r \tag{2}$$

$$\boldsymbol{E} = -\nabla \phi \tag{3}$$

where n is the electron density, $\boldsymbol{E}$ the electric field, ϕ the potential, N_D the ionized donor density, and R the recombination term, whose effect is negligible in monopolar devices (apart from breakdown conditions). Finally, q is the electron charge (taken as positive), ϵ_0 the vacuum permittivity, and ϵ_r the relative permittivity of the material. Material characteristics are described by the mobility–electric field curve $\mu = \mu(E)$, which is approximated as in [30]; the diffusivity D is related to mobility through the Einstein relation. Thermal effects due to heat generation within the active region have also been included in a more recent version of the simulator [19] but will not be discussed here. The presence of surface states is included through equivalent boundary conditions, while buffer traps are accounted for through effective donor concentration; the treatment of other boundary conditions is conventional. Since the MESFET is invariant for translation along the gate, the analysis can be confined to the two-dimensional device cross section. Three-dimensional effects mainly concern propagation along the gate, and will be discussed further on.

Both doping and low-field mobility profiles are arbitrary in MESS, thereby permitting the simulation of symmetric, unbuffered, and buffered devices. However, assigning correct mobility and doping profiles is by no means trivial. In fact, C–V measurements do not yield reliable data on the doping profile on the interface between the active and the buffer layers, which determines the cutoff characteristics of the device. On the other hand, measurements of initial mobility in the buffer layer or the transition between the active and the buffer layers are still somewhat controversial [35]. Actually, the buffer actually behaves as a low-mobility region, rather than as a high-mobility one, as Hilsum's relation between initial mobility and doping level would suggest [26]. The mobility profile in the buffer has considerable impact upon the low-field characteristics but also affects the equivalent drain and source resistances.

B. Analyzing the Device Behavior

Device simulation in steady-state, small-signal, or large-signal operating conditions is based on the numerical solution of the model (1)–(3). The *discretization* scheme implemented in MESS makes use of a two-dimensional extension on a triangular grid [6] of the Scharfetter–Gummel scheme.[1] The discretization of the Poisson equation is based on linear FEM combined with the so-called charge lumping—a first-order scheme which has some advantages with respect to the so-called consistent scheme in which the charge density is approximated linearly. The *solution* of the discretized system requires different techniques according to whether *steady-state*, *small-signal*, or *large-signal* simulation is concerned. In the approach followed in the MESS simulator, only steady-state and small-signal simulations are needed to obtain small- and large-signal circuit-oriented characterizations. Efficiency is achieved in MESS in both operating conditions (steady-state and small-signal) by means of techniques which are discussed in the next two subsections.

1) Efficient Schemes for Steady-State Simulation: The discretized Poisson continuity system in steady state (zero time derivatives) can be written as

$$\begin{bmatrix} 0 & \mathbf{C}(\phi) \\ \mathbf{A} & \alpha\mathbf{B} \end{bmatrix} \begin{bmatrix} \phi \\ \boldsymbol{n} \end{bmatrix} = \begin{bmatrix} \boldsymbol{r}_1 \\ \boldsymbol{r}_2 \end{bmatrix} \tag{4}$$

where ϕ and $\boldsymbol{n}$ are vectors of unknown potential and charge values at the N discretization nodes. The right-hand terms $\boldsymbol{r}_1, \boldsymbol{r}_2$ are derived from Dirichlet boundary conditions (see e.g. [46]); the second term also includes the donor density N_D. The matrices $\mathbf{A}, \mathbf{B}, \mathbf{C}$ have dimensions $N \times N$ and can be obtained through FEM-like element-by-element assembling as outlined in [6].

Two techniques are currently used to solve (4) (see e.g. [40]): the *coupled* scheme, in which (4) is solved by means of Newton techniques, requiring system linearization; and the *uncoupled* scheme, in which Poisson and continuity equations are alternatively and iteratively solved until convergence is achieved. The comparative merits of the two techniques when applied to MESFET's turned out to be approximately the same as in MOS simulation (see e.g. [40]): in spite of the greater cost of each iteration step (the solution of a linear system of dimension $2N$ rather than two systems of dimension N), *coupled* methods should be favored in MESFET simulation owing to their superior robustness and independence of bias conditions.

A definite improvement over conventional Newton implementations would be achieved if the rank of the system to be solved at each Newton step could be reduced from $2N$ to N. This is indeed possible if a proper discretization scheme is exploited as follows.

Let us consider again the nonlinear system arising from spatial discretization of Poisson and continuity equations. If Newton's method is applied for the solution, the iterative process takes the form

$$\boldsymbol{n}^k = \boldsymbol{n}^{k-1} + \Delta \boldsymbol{n}^k \tag{5}$$

$$\phi^k = \phi^{k-1} + \Delta \phi^k \tag{6}$$

where $\Delta \boldsymbol{n}^k, \Delta \phi^k$ are the solution to the linearized system

$$\begin{bmatrix} \mathbf{E}^{k-1} & \mathbf{C}^{k-1} \\ \mathbf{A} & \alpha\mathbf{B} \end{bmatrix} \begin{bmatrix} \Delta\phi^k \\ \Delta\boldsymbol{n}^k \end{bmatrix} = \begin{bmatrix} \boldsymbol{r}_1 \\ \boldsymbol{r}_2 \end{bmatrix} - \begin{bmatrix} 0 & \mathbf{C}^{k-1} \\ \mathbf{A} & \alpha\mathbf{B} \end{bmatrix} \begin{bmatrix} \phi^{k-1} \\ \boldsymbol{n}^{k-1} \end{bmatrix}. \tag{7}$$

The superscript $k-1$ refers to a matrix being evaluated at $\phi = \phi^{k-1}$. The matrix $\mathbf{E}$ derives from linearization with

[1] In contrast to the conventional one, the present scheme also allows for *obtuse* triangular elements.

respect to potential and also includes the derivative of the mobility-field relationship.

Now, the matrices **A**, **C**, **E** are *banded* (or *sparse*), but **B** is *diagonal* if charge lumping is employed in discretizing the Poisson equation. As a consequence, **B** can be inverted inexpensively and the Poisson equation can be solved with respect to charge density. Hence, one can write

$$\Delta \boldsymbol{n}^k = -\frac{1}{\alpha}\mathbf{B}^{-1}\mathbf{A}\left(\Delta\boldsymbol{\phi}^k + \boldsymbol{\phi}^{k-1}\right) + \frac{1}{\alpha}\mathbf{B}^{-1}\boldsymbol{r}_2 - \boldsymbol{n}^{k-1} \quad (8)$$

and, expressing in the first equation the charge density variation as a function of potential variation, one has

$$\left[\mathbf{E}^{k-1} - \frac{1}{\alpha}\mathbf{C}^{k-1}\mathbf{B}^{-1}\mathbf{A}\right]\Delta\boldsymbol{\phi}^k = -\frac{1}{\alpha}\mathbf{C}^{k-1}\mathbf{B}^{-1}\boldsymbol{r}_2 + \frac{1}{\alpha}\mathbf{C}^{k-1}\mathbf{B}^{-1}\mathbf{A}\boldsymbol{\phi}^k + \boldsymbol{r}_1. \quad (9)$$

Once (9) is solved with respect to $\Delta\boldsymbol{\phi}^k$ the charge variation is obtained at the cost of the product between a banded matrix and a vector, thereby reducing the cost of one Newton step to (approximately) the factorization of a banded matrix of rank N. One iteration with the scheme given by (8) and (9) (fast coupled, FC) thus appears to be less expensive than with the usual Newton implementation (ordinary coupled, OC) and comparable to one decoupled iteration (ordinary uncoupled, OU). Careful examination reveals however that some price has to be paid also in FC, since the banded matrices appearing in (9) have a bandwidth which is *twice* as large as the original matrices **A**, **E**, **C**. Supposing that a banded LU factorization–back substitution technique is used for all cases, and neglecting speedup techniques such as Newton–Richardson (which can be applied both to OC and FC), one has to solve each iteration step: two systems of rank N, total bandwidth B for OU; one system of rank $2N$, total (approximate) bandwidth $2B$ for OC;[2] one system of rank N, total bandwidth $2B$ for FC. Now, defining ν as the cost of the FORTRAN operation Y(I) = Y(I) + T * X(I), and taking into account that the cost of a system solution is approximately $(2NB^2 + 3NB)\nu$, (N system rank, B bandwidth) [12], where the first term in brackets (factorization) is currently dominant with respect to the second (back-substitution), the iteration cost is $\approx 4NB^2\nu$ for OU, $\approx 16NB^2\nu$ for OC, and $\approx 8NB^2\nu$ for FC. The fast coupled scheme is approximately twice as fast as the ordinary coupled scheme and is certainly faster than the uncoupled one, since only ten iterations are typically needed with the coupled Newton–Richardson schemes, of which only three or four require factorization, as against the 20–50 iterations of the uncoupled schemes. Experience over a variety of cases shows that, for the number of unknowns needed for simulating ordinary MESFET devices (1000–2000), the fast coupled approach is not only more reliable, but also significantly faster than the uncoupled approach. Furthermore, a polynomial scheme has been implemented to extrapolate the starting point of Newton's iteration from the already computed solutions. This scheme enables the computation of the $V-I$ characteristics to be considerably sped up, thereby reducing the average cost of a bias point to fewer than two factorizations and to three to five back substitutions.

[2] It can be shown that if B is the optimum bandwidth for Poisson and continuity equations, $2B$ is a quasi-optimum bandwidth for the OC system.

A complete example of *steady-state* simulation for an implanted half-micron MESFET (TELETTRA) is presented in Fig. 2. The layout of the device is shown in Fig. 2(a); the doping and initial mobility profile are seen in Fig. 2(b) and (c). In Fig. 2(d) the measured static $V-I$ curves (dots) are compared to the simulated ones (solid lines). Finally, a set of internal distributions (potential, charge, electric field, current density) is shown in Fig. 2(e) for $V_d = 4$ V, $V_g = -2$ V (device near pinch-off).

2) Efficient Schemes for Small-Signal Simulation: The small-signal response can be obtained either by applying "small" inputs to a large-signal time-domain model [37] or by linearizing the model equations around a working point [29]. The former approach has been widely followed in the past, but presents two difficulties: first, the input signals must be small enough not to introduce nonlinearity but large enough to make the response free from numerical noise; second, the time evolution of the device has to be computed by means of a time-consuming large-signal model. Therefore, direct linearization has been employed in this research. The linearized Poisson continuity system reads

$$\frac{\partial \delta n}{\partial t} = \nabla\cdot\left[\delta n\mu(E_0)\mathbf{E}_0 + n_0\mu(E_0)\delta\mathbf{E} + n_0\mu'(E_0)\delta E\,\mathbf{E}_0 + D(E_0)\nabla\delta n + D'(E_0)\delta E\nabla n_0\right] \quad (10)$$

$$\nabla^2\delta\phi = \alpha\delta n \quad (11)$$

$$\delta\mathbf{E} = -\nabla\delta\phi \quad (12)$$

where the subscript 0 refers to the working point value, while δn, $\delta\phi$, and $\delta\mathbf{E}$ are variations with respect to the working point. The symbols μ' and D' refer to the derivatives of mobility and diffusivity with respect to the electric field. If the discretization algorithm already discussed for the steady state analysis is applied to (10) and (11) (or, equivalently, if the large-signal discretized equations are linearized around a working point), one has the system

$$\mathbf{E}\delta\boldsymbol{\phi}(t) + \mathbf{C}\delta\boldsymbol{n}(t) + \mathbf{B}\frac{d\delta\boldsymbol{n}(t)}{dt} = 0 \quad (13)$$

$$\mathbf{A}\delta\boldsymbol{\phi}(t) + \alpha\mathbf{B}\delta\boldsymbol{n}(t) = \boldsymbol{r}_3(t) \quad (14)$$

where the matrices **E** and **C** are evaluated at the working point and the arrays $\delta\boldsymbol{\phi}(t)$ and $\delta\boldsymbol{n}(t)$ represent nodal values. Note that $\boldsymbol{r}_3(t)$ depends only on boundary conditions.

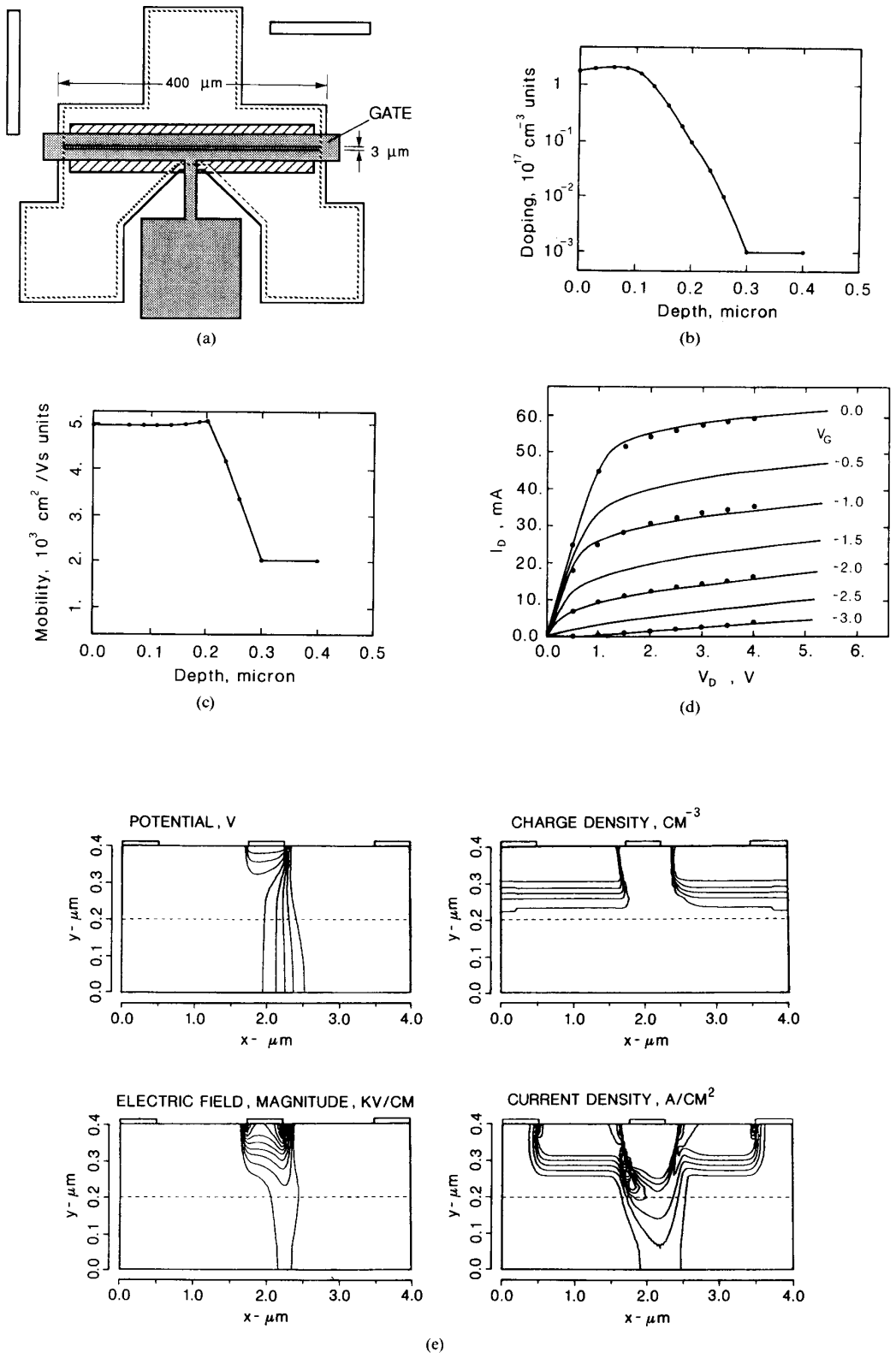

Fig. 2. (a) Layout of half micron gate implanted MESFET (Courtesy of TELETTRA). (b) Doping profile for the device of Fig. 2(a). (c) Initial mobility profile for the device of Fig. 2(a). (d) Static $V-I$ curves for the device of Fig. 3(a). Continuous lines are simulated results, dots represent measurements (Courtesy of TELETTRA). Lead resistances of 1 Ω simulating text fixture contact resistances have been added to the model. (e) Internal field distributions for the implanted device of Figs. 2(a)–(d). The working point is $V_s = 0$, $V_g = -2$, $V_d = 4$ V. (*upper left*) Potential: $\Delta V = 0.74$ V. (*upper right*) Charge density: $\Delta n = 0.38 \times 10^{17}$ cm^{-3}. (*lower left*) Magnitude of the electric field: $\Delta E = 62.1$ kV/cm. (*lower right*) Magnitude of current density: $\Delta J = 91.0$ kA/cm^2.

Two techniques can be used to solve system (13), (14). In the *first approach* the system is Fourier transformed and solved in the frequency domain. In this case one has to solve, for each frequency, a *complex* system of dimension $2N$, so that the solution for M frequencies requires M factorizations. Although block iteration techniques have been proposed to solve the system without having to factorize a complex matrix of rank $2N$, direct factorization is needed for high frequencies [29].

In the *second approach*, which has been followed here, the system given by (13) and (14) is solved in the time domain by means of a suitable quadrature scheme. Two step excitations are applied, to the drain and gate, respectively, and the resulting time-domain response is Fourier transformed by means of FFT algorithms.

Using as a quadrature rule a backward Euler scheme, which is unconditionally stable and permits easy error monitoring and time step adjustment [1], and taking into account the properties of the matrices $\mathbf{A},\mathbf{B},\mathbf{C},\mathbf{E}$, we can apply to the time-discretized version of system (13), (14) the rank reduction technique already described for the steady-state simulation. This gives

$$\delta \boldsymbol{n}(t+\Delta t) = \frac{1}{\alpha}\mathbf{B}^{-1}\boldsymbol{r}_3 - \frac{1}{\alpha}\mathbf{B}^{-1}\mathbf{A}\delta\phi(t+\Delta t) \quad (15)$$

$$\left[\frac{1}{\alpha}\mathbf{C}\mathbf{B}^{-1}\mathbf{A} + \frac{1}{\alpha\Delta t}\mathbf{A} - \mathbf{E}\right]\delta\phi(t+\Delta t) = \frac{1}{\alpha}\left[\mathbf{C}\mathbf{B}^{-1} + \frac{1}{\Delta t}\mathbf{I}\right]\boldsymbol{r}_3 + \frac{1}{\Delta t}\mathbf{B}\delta\boldsymbol{n}(t). \quad (16)$$

Let us briefly discuss the computational efficiency of the *time-domain* versus the *frequency-domain* small-signal analysis technique. If we define n_T as the number of time steps required to perform the time-domain simulation (TD) and n_F as the number of frequency domain (FD) samples and introduce as a basic performance index the parameters ν_R (real arithmetic) and ν_C (complex arithmetic), the cost of a small-signal analysis amounts to $n_F(16NB^2+12NB)\nu_C$ for FD (n_F factorizations and substitutions) to $(8NB^2+6n_TNB)\nu_R$ for TD (one factorization and n_T substitutions). We suppose that in both cases a *fast coupled* technique is used, and neglect the additional cost of FFT in TD. Although the ratio between ν_C and ν_R is machine dependent, a reasonable estimate for a computer where complex arithmetic has been somewhat optimized is $\nu_C/\nu_R \approx 3$. If this estimate is taken into account and normalized with respect to ν_R, the cost will be $24n_FNB^2$ for the FD simulation and $6n_TNB$ for the TD simulation. In order to obtain the same computer cost, one should have $n_T = 4Bn_F$. Since bandwidth values of 20–30 are common and n_T usually has values ranging from one to several hundred, it is clear that frequency-domain simulation is convenient only when a small number of frequency samples (say, fewer than 10) are required.

Although this analysis holds only for a constant time integration step, our experience shows that no appreciable performance deterioration is caused by variable step integration schemes. Indeed, considerable computer time saving can be achieved in many cases, although for GaAs devices the need for variable step algorithms is not as stringent as it is in MOS or bipolar simulation. Hence, we can conclude that the time integration scheme seems to have definite advantages with respect to the frequency-domain one if the entire frequency response of the device has to be computed. An advantage of the FD scheme is that greater accuracy can be achieved; however, in our experience the computational accuracy of TD simulation is acceptable in most practical cases.

By using the small-signal TD simulator, the pulse responses of the MESFET to input and output pulse voltage excitations can be easily computed; on this basis the Y matrix of the "intrinsic" device (i.e., the part of the device considered in the 2-D simulation) can be obtained by fast Fourier transform techniques following an approach similar to that in [37].[3]

C. Predicting Microwave Performance: Propagation Effects and External Parasitics

Owing to its CPU intensity, physical simulation is limited to the intrinsic device or little more; other phenomena related to the three-dimensional nature of the device (propagation along the gate, lead inductances, and, above all, matching networks needed in microwave applications) have to be accounted for through proper postprocessing of the data derived from physical simulation.

Propagation effects are included in MESS through a technique described in greater detail in [20]. Basically, the MESFET is modeled as a multiconductor transmission line whose parameters (per-unit-length *admittance* $\mathscr{Y}$ and *impedance* $\mathscr{Z}$) are evaluated partly from *physical simulation* and partly from *electromagnetic models*. Namely, for a device having M active regions (i.e., gate pads),

$$\mathscr{Y} = \sum_{i=1}^{M} \mathbf{Y}_{ai}(\omega) + j\omega(\mathbf{C}_{\text{int}} + \mathbf{C}_{\text{ext}}) \quad (17)$$

$$\mathscr{Z} = \mathbf{R}(\omega) + j\omega\mathbf{L}_{\text{tot}} \quad (18)$$

where $\mathbf{Y}_{ai}$ is the per-unit-length admittance matrix of the ith active region, computed from the small-signal physical model; $\mathbf{C}_{\text{int}}$ and $\mathbf{C}_{\text{ext}}$ are the internal (substrate) capacitance and the external (air) capacitance per unit length; $\mathbf{R}$ is the per-unit-length frequency-dependent resistance matrix of the electrodes, and $\mathbf{L}_{\text{tot}}$ is their overall per-unit-length inductance. The admittance matrix of the distributed model can be obtained through standard multiconductor line analysis; details are omitted for the sake of brevity. The validity of a lossy transmission line electromagnetic model has been confirmed by the results of a recent full-wave analysis which, owing to its complexity, is

[3]Note, however, that in [37] a large-signal model with "small" inputs is used to obtain the small-signal time-domain response.

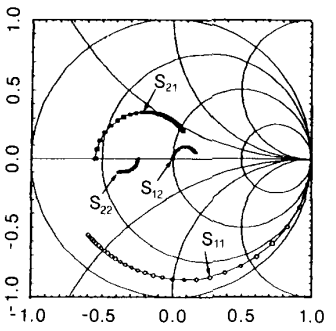

Δf = 1.0 GHz S_{21} scaled by 2.0

(a)

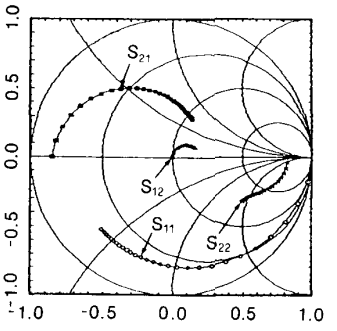

Δf = 1.0 GHz S_{21} scaled by 3.0

(b)

Fig. 3. Simulated scattering parameters with respect to 50 Ω for the same device as in Fig. 2(a)–(e). 1 and 2 stand for gate and drain electrodes, respectively. Distributed gate effects are included. The source and gate voltages are $V_s = 0$, $V_g = 0$ V for all working points. (a) $V_d = 0.5$ V (linear region); (b) $V_d = 3.0$ V (saturation). The frequency spacing between points is 1 GHz.

limited to considering a single-gate MESFET and uses a rather crude model to simulate the active region of the device [23], [24]. The technique proposed here enables the exploitation of an accurate wide-band characterization derived from physical simulation to model the active region, rather than a simplified lumped-parameter model, as in [28], [38], [34], and [24].

An example of small-signal simulation is shown in Fig. 3(a) and (b) for the same device as in Fig. 2, where the (computed) scattering matrix of the device is presented for two working points ($V_g = 0$, V_d in the linear region and in saturation). Comparisons with measured S parameters suggest that the agreement is good provided that air and substrate parasitic capacitances are properly included in the model. This point is discussed in detail in [17], with reference to a 1 μm device measured over the range 5–15 GHz.

Finally, to the S parameter characterization thus obtained, external parasitics can be added as circuit elements by means of a circuit simulator. It is therefore clear that accurate characterization of the *isolated* (e.g. *discrete*) device already requires the possibility of interfacing physical and circuit simulation, which will be discussed in greater detail in the next section.

III. Linking Physical and Circuit Simulation

As outlined in the Introduction, an intermediate link is needed between the physical model, mainly oriented to device technology, and the performance prediction under practical operating conditions, which can be more conveniently dealt with through circuit-level simulation. The MESS simulator already provides an S (or Y) parameter frequency-domain characterization of the MESFET which is sufficient for performance prediction in any small-signal application; in particular, the output file can be formatted according to SUPERCOMPACT standards as well as for the in-house-developed ACCAD [4].

A slightly different link to circuit simulators can be obtained under the form of *equivalent circuits* for both *small-signal* and *large-signal* operation. Indeed, the possibility of obtaining large-signal characterizations based on physical models without actually needing a large-signal analysis performed on the physical model itself is one of the most appealing features of the present approach. In fact, most equivalent circuit models [31], [36], [3] are identified, even in the large-signal case, in terms of dc characteristics and small-signal Y or S parameters measured for several different bias conditions. Since these are the basic results provided by a physical model, the same measurement-oriented identification procedures can be used to derive an equivalent circuit from physical device simulations. However, the amount of information offered by physical simulation is much greater than direct measurement can provide, since the values of electrical variables *inside* the device are also made available; these in particular can be conveniently used for easier and more accurate identification of a circuit model, besides yielding better understanding and suggesting possible improvements in its structure.

A. Small-Signal Equivalent Circuit

Though not strictly necessary for small-signal characterization, a relatively simple lumped equivalent circuit [31] (see e.g. Fig. 4(a)), is a useful tool not only for circuit design purposes but also for the direct evaluation of the RF amplifying capabilities of the device; moreover, it is a first step in the development of a large-signal equivalent circuit.

The circuit model in Fig. 4(a) could be characterized according to classical measurement-oriented parameter fitting procedures. However, owing to the additional information on internal electrical variables made available by the physical simulator, a more straightforward parameter extraction procedure can be used. In fact, since also the voltages v_g', v_d', v_s' in the intrinsic transistor[4] are obtained (in addition to the gate and source currents) from the

[4]Some suitable points in the two-dimensional simulation can be chosen as intrinsic source s', drain d', and gate g'. A more complete strategy for the identification of resistive regions within the device, based on direct analysis of the field distribution, will be presented in [21].

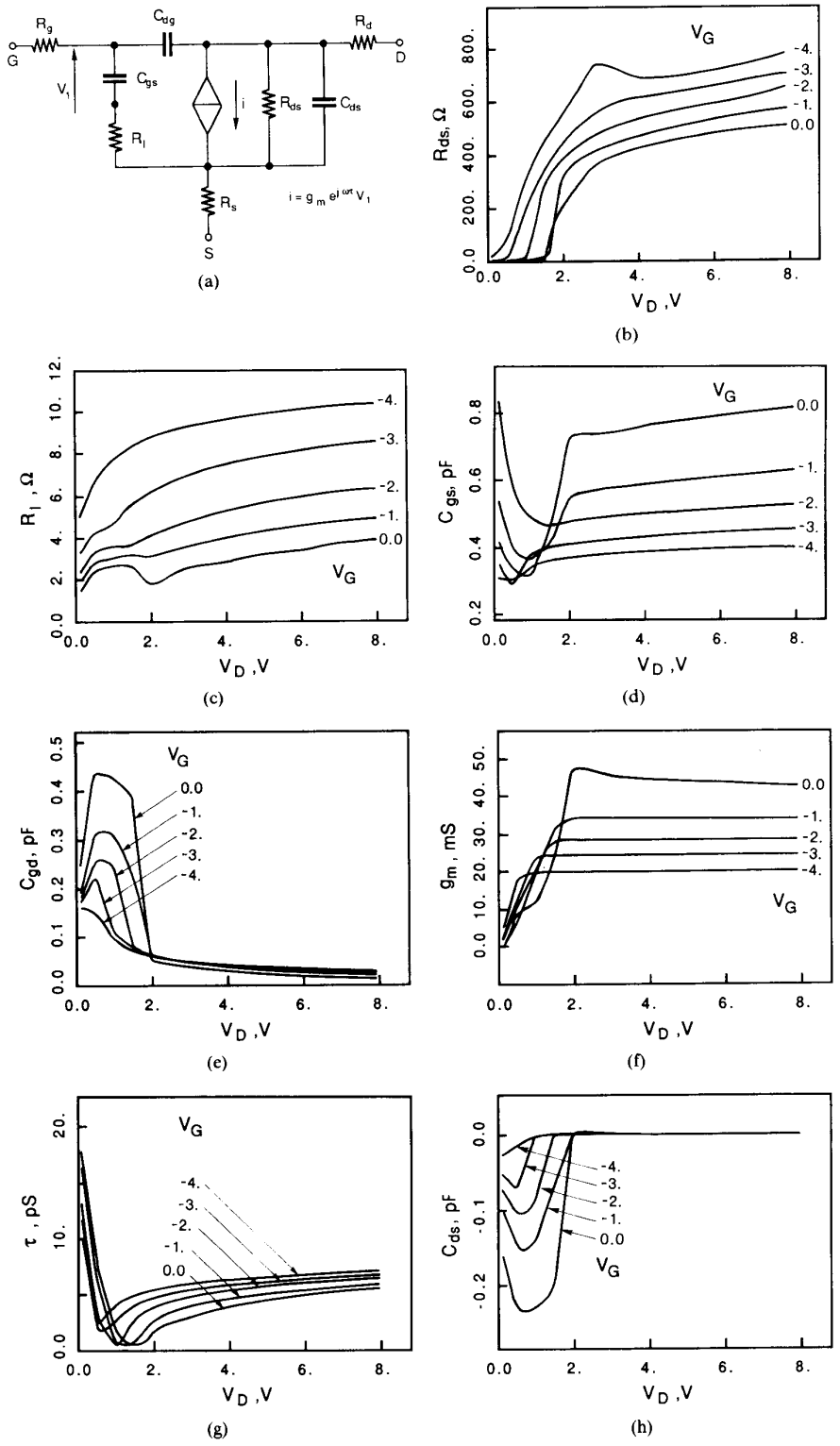

Fig. 4. (a) Small-signal equivalent circuit. Variation of small-signal parameters as a function of working point: (b) R_{ds}, (c) R_I, (d) C_{gs}, (e) C_{gd}, (f) g_m, (g) τ, and (h) C_{ds}. R_d and R_s are almost constant and can be assumed to take on the average values $R_d = 7\ \Omega$, $R_s = 2.5\ \Omega$.

transient simulations, the values of the parasitic resistances R_s, R_d, R_g can be computed according to the equations

$$R_s = \{v_s - v_{s'}\}/\{i_s\} \tag{19}$$

$$R_d = \{v_d - v_{d'}\}/\{i_d\} \tag{20}$$

$$R_g = \{v_g - v_{g'}\}/\{i_g\} \tag{21}$$

where

$$\{\bullet\} = \sqrt{\frac{1}{T}\int_0^T (\bullet)^2\, dt} \tag{22}$$

T being the practically finite duration of the pulse response. In (19)–(21) the r.m.s. values are considered instead of the instantaneous values, in order to introduce a suitable averaging of the electrical variables over the transient interval. Thus the admittance matrix $\mathbf{Y}'$ of the intrinsic device can be computed for any angular frequency ω by "subtracting" (according to the well-known formulas for linear multiport connection) the contributions due to resistances R_s, R_d, and R_g from the $\mathbf{Y}$ matrix of the whole chip. Finally, taking into account the relation between the equivalent circuit and the matrix $\mathbf{Y}$, the parameter values can be computed by using the inverse formulas:

$$C_{gd} = -\operatorname{Im}(Y'_{gd}/\omega) \tag{23}$$

$$R_I = \operatorname{Re}\left(\frac{1}{Y'_{gg} - j\omega C_{gd}}\right) \tag{24}$$

$$1/C_{gs} = -\omega \operatorname{Im}\left(\frac{1}{Y'_{gg} - j\omega C_{gd}}\right) \tag{25}$$

$$g_m \exp(-j\omega\tau) = (Y'_{dg} + j\omega C_{gd})(1 + j\omega R_I C_{gs}) \tag{26}$$

$$R_{ds} = 1/\operatorname{Re}(Y'_{dd}) \tag{27}$$

$$C_{ds} = \operatorname{Im}(Y'_{dd})/\omega - C_{gd}. \tag{28}$$

If the model were exact, the circuit parameters would be frequency independent. However, owing to the intrinsic simplifications of lumped models, some slight frequency dependence may arise; thus, if broad-band operation has to be considered, some parameter fitting could be needed. This, in practice, may consist of a simple averaging of the parameter values over the frequency range concerned. Since the equivalent circuit parameters are bias dependent, useful information is provided not only for the optimal choice of the bias but also for the identification of the most important nonlinear effects to be taken into account when deriving a large-signal model.

B. Large-Signal Equivalent Circuit

In the *large-signal* case the identification of a nonlinear equivalent circuit is an essential tool for predicting the transistor performance under realistic operating conditions, generally involving a relatively complex external

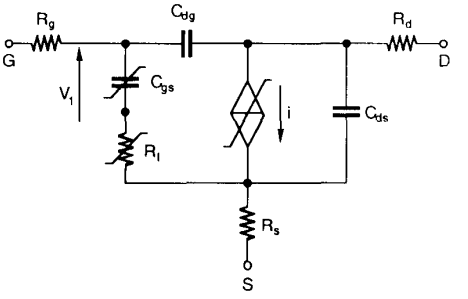

Fig. 5. Large-signal model derived from the small-signal model of Fig. 4(a). One has $i(t) = f[v_1(t-\tau), v_2(t)]$, $C_{gs} = C_{gs}(v_1)$, $R_I = R_I(v_1)$.

circuit. Whenever the nonlinear characteristics of the MESFET are crucial in a particular application (e.g. power amplifiers, oscillators, frequency converters, etc.), the only practical way to compute the in-circuit performance consists of deriving a nonlinear equivalent circuit compatible with a nonlinear circuit analysis code such as PSPICE, QSS [14], [32], or QND [33] or the vectorized code described in [39]. To this aim, most of the CAD-oriented equivalent circuits, which can be characterized by dc and small-signal S matrix measurements, can be directly used. However, two slightly different approaches can be followed.

In the first [36], [3] the structure and nonlinear characteristics of the large-signal model are derived from the bias dependence of the parameters of a small-signal one. If the equivalent circuit in Fig. 4(a) is considered, the results of the physical simulation shown in Fig. 4(b)–(h) point out that the most relevant bias dependence (i.e., nonlinearity) is associated with C_{gs}, R_I, g_m, and R_{ds}; the other elements can be assumed to be practically linear. The parameters shown in Fig. 4(b)–(h) refer to the device whose experimental parameter values are reported in [44]. In spite of the lack of complete information on the doping profile and on the geometrical dimensions of this device, good qualitative agreement can be noticed between simulated and measured results. On this basis, the large-signal equivalent circuit shown in Fig. 5 is obtained, where the dependence of C_{gs} and R_I on v_1 only is assumed since the plots in Fig. 4(b)–(h) show a stronger dependence on the bias voltage V_{gs}, while the dependence on V_{ds} is smaller. Considering that in dc operation $v_1 \approx V_{gs}$, $v_2 \approx V_{ds}$ these plots directly characterize the nonlinear dependence of C_{gs}, R_I and of the controlled current source f on the controlling voltages v_1, v_2. The function f can be obtained by integrating the differential parameters g_m and R_{ds}, according to the technique in [36] and [3].

This procedure for the identification of large-signal circuit models for GaAs MESFET's via 2-D physical simulation has been adopted in the analysis and design of a monolithic power MESFET feedback amplifier [22]. In particular, the nonlinear model in Fig. 5 has been used for the large-signal amplifier analysis by means of the harmonic balance method and for the optimization of the

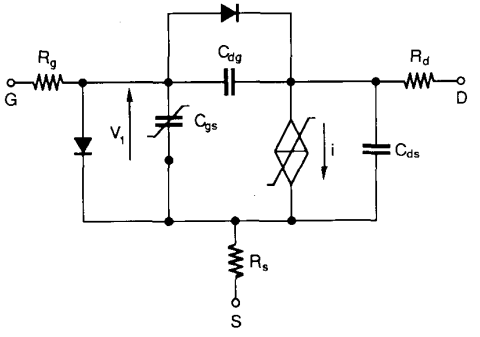

Fig. 6. A simple large-signal model for GaAs MESFET's. One has $i(t) = F[v_1(t-\tau), v_2(t)]$, $C_{gs} = C_{gs}(v_1)$, $C_{gd} = C_{gd}(v_1 - v_2)$.

circuit performance by means of numerical minimization techniques (QND).

In another, slightly different approach, a suitable structure for the large-signal model is first defined and the nonlinear characteristics are then derived by fitting its dc and small-signal RF behavior for a large set of different bias conditions on the corresponding results obtained from physical simulations. For instance, we may consider the simple large-signal equivalent circuit shown in Fig. 6, where the dc characteristics are modeled by a nonlinear voltage-dependent current source (including also transit time phenomena) and two diodes which take into account the possible conduction (in large-signal RF operation) of the gate junction; charge storage effects are described in terms of voltage-dependent capacitors. The characteristics of these nonlinear elements can be approximated by suitable functions as, for instance, the simple relationships used in the PSPICE circuit simulation program [10], whose parameters can be derived by numerical minimization of the mean-square discrepancy between the S matrices and dc characteristics of the equivalent circuit and those obtained from the physical simulations. This procedure has been applied to the modeling of a MESFET device to be used as the active element in a dielectric resonator oscillator [15]; in this case, the time-domain circuit simulator SPICE was used instead of a harmonic balance algorithm, since not only the periodic steady-state, but also the transient response had to be computed in order to verify the "self-starting" behavior of the oscillator.

Finally, we would like to point out that physical simulation opens new possibilities in the domain of large-signal equivalent circuits. First, physical simulation performed for a large number of bias conditions yields an almost complete "sampled" characterization for the voltage-dependent functions describing the nonlinear equivalent circuit. Such data could be directly used (via numerical interpolation) by the large-signal circuit simulator. Second, the results from physical simulation allow the adoption of more accurate, though more complex, equivalent circuits whose identification would be difficult if only measurements at the external ports were available. For instance, the more accurate circuit model of Fig. 7 can be used, where the distributed nonlinear $R-C$ structure of the

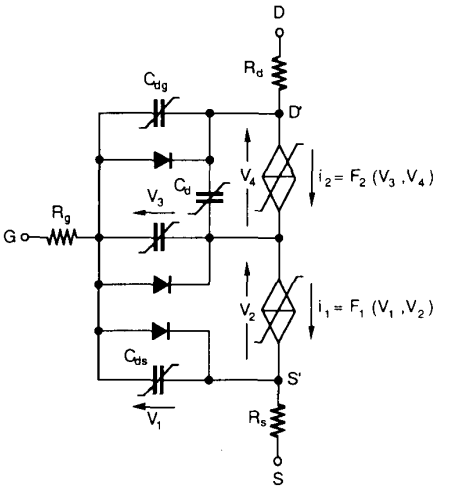

Fig. 7. Large-signal GaAs MESFET model consisting of two lumped nonlinear $R-C$ 3-poles.

actual MESFET is approximated by two lumped nonlinear $R-C$ 3-poles instead of a single one as in Fig. 6. This more complex model would be difficult to characterize only in terms of "external" measurements, even if the simplified analytical formulas proposed in [8] were used to describe the nonlinear elements; however, the task of identifying this model becomes easier if the values of internal electrical variables, such as the voltage v_A or the current i_1[5] are made available by physical simulation in addition to the voltages v_g, v_d, v_s. This approach, which is a physical-simulation-based method for the topological and parameter identification of large-signal equivalent circuits of GaAs MESFET's, will be described in greater detail in [21].

IV. Conclusions

An approach has been proposed to obtain an integrated CAD environment allowing microwave devices to be simulated from the technological stage to circuit level. Its key points are an efficient physical simulation code, whose features have been briefly reviewed, and its linkage to linear and nonlinear circuit analysis CAD tools. It has been shown how circuit-oriented models for small-signal analysis derived from physical simulation are useful not only for simulating the device in circuit environment, but also for accounting for external parasitics and propagation. Particular attention was paid to large-signal models, which enable large-signal physical simulation to be performed with a high degree of computational efficiency. Moreover, the new possibilities for the identification of circuit-oriented models offered by the knowledge of the internal behavior of the device made available by physical models have been preliminarily explored; further investigations on their practical implementation are currently being carried out.

[5]This implies the choice of a "cross section" which divides the device into two parts corresponding to the two lumped $R-C$ 3-poles in the equivalent circuit.

ACKNOWLEDGMENT

The authors are indebted to the technical staff of TELETTRA for providing technical information on MESFET devices and for helpful discussions.

REFERENCES

[1] R. E. Bank *et al.*, "Transient simulation of silicon devices and circuits," *IEEE Trans. Electron Devices*, vol. ED-32, pp. 1992–2006, Oct. 1985.

[2] T. M. Barton, C. M. Snowden, and J. R. Richardson, "The effect of surface, gate, and buffer on the operation of GaAs MESFETs," presented at the 3rd Meeting of GaAs Simulation Group, Duisburg, West Germany, 7–8 Oct. 1986.

[3] G. P. Bava *et al.*, "Non-linear simulation of power GaAs MESFETs," *Modelling, Simulation & Control*, part A, vol. 1, no. 2, pp. 7–22, Feb. 1984.

[4] C. Beccari and C. Naldi, "ACCAD, a new microwave circuit CAD package," in *Proc. Int. Symp. Microwave Technol. Ind. Develop.* (Campinas, Brazil), July 1985, pp. 269–273.

[5] K. Bløtekjær, "Transport equations for electron in two-valley semiconductors," *IEEE Trans. Electron Devices*, vol. ED-17, pp. 38–47, Jan. 1970.

[6] E. M. Buturla, P. E. Cottrell, B. M. Grossman, K. A. Salsburg, "Finite element analysis of semiconductor devices: The FIELDAY program," *IBM J. Res. Develop.*, vol. 25, no. 4, pp. 218–231, July 1981.

[7] E. Caquot *et al.*, "Integration of process, device and circuit models for III–IV devices," *The Interfaces and Integration of Process Device and Circuit Models — An Introduction*, J. J. H. Miller, Ed. *Proc. Short Course*, *NASECODE V Conf.* (Dublin), June 1987, pp. 8–18.

[8] L. O. Chua and Y. W. Sing, "Nonlinear lumped circuit model of GaAs MESFET," *IEEE Trans. Electron Devices*, vol. ED-30, pp. 825–833, July 1983.

[9] R. K. Cook and J. Frey, "An efficient technique for two-dimensional simulation of velocity overshoot effects in Si and GaAs devices," *COMPEL*, vol. 1, no. 2, pp. 65–87, 1982.

[10] W. R. Curtice, "A MESFET model for use in the design of GaAs integrated circuits," *IEEE Trans. Microwave Theory Tech.*, vol. MTT-28, pp. 448–456, May 1980.

[11] W. R. Curtice and Y. H. Yun, "A temperature model for the GaAs MESFET," *IEEE Trans. Electron Devices*, vol. ED-28, pp. 954–962, Aug. 1981.

[12] J. J. Dongarra, J. R. Bunch, C. B. Moler, and G. W. Stewart, *LINPACK User's Guide*, SIAM, 1979.

[13] Y. K. Feng, "New $v(E)$ relationship for GaAs," *Electron. Lett.*, vol. 21, no. 10, pp. 453–454, 9th May 1985.

[14] F. Filicori, V. Monaco, and C. Naldi, "Simulation and design for microwave class-C amplifiers through harmonic analysis," *IEEE Trans. Microwave Theory Tech.*, vol. MTT-27, pp. 1043–1051, Dec. 1979.

[15] F. Filicori, V. Monaco, U. Pisani, and V. Pozzolo, "Progettazione di oscillatori con risonatore dielettrico a microonde con tecniche CAD," in *Proc. LXXXVIII Riun. Ann. AEI* (Catania), 27–30 Sept. 1987, pp. 3B5.1–7.

[16] G. Ghione, R. D. Graglia, C. Naldi, and G. P. Donzelli, "Two-dimensional device simulation as a tool for the development of microwave power GaAs MESFETs," in *Proc. Int. AMSE Conf.* Sorrento (Italy), 1986, vol. 2.1, pp. 121–133.

[17] G. Ghione, C. U. Naldi, F. Filicori, M. Cipelletti, and G. Locatelli, "MESS—A two-dimensional physical device simulator and its application to the development of *C*-band power GaAs MESFET's," *Alta Frequenza*, vol. LVII, pp. 295–309, Sept. 1988.

[18] G. Ghione and C. Naldi, "MESS—A finite element steady state and small-signal MESFET simulator," presented at the 3rd Meeting of GaAs Simulation Group, Duisburg, West Germany, 7–8 Oct. 1986.

[19] G. Ghione, P. Golzio, and C. Naldi, " Thermal analysis of power GaAs MESFETs," in *Proc. NASECODE V* (Dublin), June 1987, pp. 195–200.

[20] G. Ghione and C. Naldi, "Modeling and simulation for wave propagation effects in MESFET devices based on physical models," in *Proc. ESSDERC '87* (Bologna), Sept. 1987, pp. 317–320.

[21] G. Ghione, C. Naldi, and F. Filicori, "Identification of large-signal equivalent circuits of GaAs MESFETs from physical simulation," in preparation.

[22] G. Ghione, C. Naldi, and F. Filicori, "A new, circuit-oriented CAD approach for the small-and large-signal simulation of GaAs MESFETs based on physical models," in *Proc. 17th European Microwave Conf.* (Rome), Sept. 1987, pp. 605–610.

[23] W. Heinrich and H. L. Hartnagel, "Wave propagation on MESFET electrodes and its influence on transistor gain," *IEEE Trans. Microwave Theory Tech.*, vol. MTT-35, pp. 1–8, Jan. 1987.

[24] W. Heinrich, "Distributed equivalent-circuit model for traveling-wave FET design," *IEEE Trans. Microwave Theory Tech.*, vol. MTT-35, pp. 487–491, May 1987.

[25] F. Heliodore, M. Lefebvre, G. Salmer, and O. El-Sayed, "Modeling of surface depletion effects in submicron MESFETs," presented at the 3rd Meeting of GaAs Simulation Group, Duisburg, West Germany, 7–8 Oct. 1986.

[26] C. Hilsum, "Simple empirical relationship between mobility and carrier concentration," *Electron. Lett.*, vol. 10, no. 13, pp. 259–260, 27 June 1974.

[27] C. Jacoboni and L. Reggiani, "The Monte Carlo method for the solution of charge transport in semiconductors with applications to covalent materials," *Rev. Mod. Phys.*, vol. 55, no. 3, pp. 645–705, July 1983.

[28] R. L. Kuvas, "Equivalent circuit model of FET including distributed gate effects," *IEEE Trans. Electron Devices*, vol. ED-27, pp. 1193–1195, June 1980.

[29] S. E. Laux, "Techniques for small-signal analysis of semiconductor devices," *IEEE Trans. Electron Devices*, vol. ED-32, pp. 2028–2037, Oct. 1985.

[30] S. E. Laux and R. J. Lomax, "Numerical investigation on mesh size convergence rate of the finite element method in MESFET simulation," *Solid-State Electron.*, vol. 24, pp. 485–493, 1981.

[31] C. Liechti, "Microwave field effect transistor 1976," *IEEE Trans. Microwave Theory Tech.*, vol. MTT-24, pp. 279–300, June 1976.

[32] C. Naldi and F. Filicori, "QSS—Quick steady state analysis program," European Space Agency Rep. No. 3334/77B, pt. 2, Jan. 1980.

[33] C. Naldi and F. Filicori, "Computer aided design of GaAs MESFET power amplifiers," in *Proc. 11th European Microwave Conf.* (Helsinki, Finland), Sept. 1982, pp. 435–440.

[34] C. H. Oxley and A. J. Holden, "Simple models for high-frequency MESFETs and comparison with experimental results," *Proc. Inst. Elec. Eng.*, vol. 133, pt. H, no. 5, pp. 335–340, 1986.

[35] M. Pillan, F. Vidimari, and A. M. Orsucci, "Dependence of mobility profiles on doping transition and impurity concentration in GaAs FET structures," in *Proc. 4th Conf. Semi-insulating III–V Materials* (Hakone, Japan), May 1986, pp. 137–141.

[36] C. Rauscher and H. A. Willing, "Simulation of nonlinear microwave FET performance using a quasi-static model," *IEEE Trans. Microwave Theory Tech.*, vol. MTT-27, pp. 834–840, Oct. 1979.

[37] M. Reiser, "A two-dimensional numerical FET model for dc, ac, and large signal analysis," *IEEE Trans. Electron Devices*, vol. ED-20, pp. 35–45, Jan. 1973.

[38] Y. A. Ren and H. L. Hartnagel, "Wave propagation studies on MESFET electrodes," *Int. J. Electron.*, vol. 51, no. 5, pp. 663–668, 1981.

[39] V. Rizzoli, C. Cecchetti, and A. Neri, "Supercomputer-aided generalized mixer analysis and optimization," in *Proc. 16th European Microwave Conf.* (Dublin), Sept. 1986, pp. 692–697.

[40] S. Selberherr, *Analysis and Simulation of Semiconductor Devices*. Vienna: Springer Verlag, 1984.

[41] C. M. Snowden, "Computer-aided design of MMICs based on physical device models," *Proc. Inst. Elec. Eng.*, vol. 133, pt. H, no. 5, pp. 419–427, Oct. 1986.

[42] C. M. Snowden and D. Loret, "Two-dimensional hot-electron models for short-gate-length GaAs MESFET's," *IEEE Trans. Electron Devices*, vol. ED-34, pp. 212–223, Feb. 1987.

[43] C. M. Snowden, M. J. Howes, and D. V. Morgan, "Large signal modeling of GaAs MESFET operation," *IEEE Trans. Electron Devices*, vol. ED-30, pp. 1817–1824, Dec. 1983.

[44] H. A. Willing, C. Rauscher, and P. de Santis, "A technique for predicting large-signal performance of a GaAs MESFET," *IEEE Trans. Microwave Theory Tech.*, vol. MTT-26, pp. 1017–1023, Dec. 1978.

[45] K. Yamaguchi, S. Asai, and H. Kodera, "Two-dimensional numerical analysis of stability criteria of GaAs FET's," *IEEE Trans. Electron Devices*, vol. ED-23, pp. 1283–1290, Dec. 1976.

[46] O. C. Zienkiewicz, *The Finite Element Method in Engineering Science*. London: McGraw-Hill, 1971.

Giovanni Ghione (M'87) was born in Alessandria in 1956. He received the Dr.Ing. degree in electronic engineering from the Politecnico di Torino, Torino, Italy, in 1981.

From 1983 to 1987 he was with the Department of Electronics of the same Politecnico as a researcher; in 1987 he joined the Politecnico di Milano as an Associate Professor. His current research activities concern the modeling of passive and active components for MMIC's (coplanar and multiconductor lines, two-dimensional physical modeling of MESFET devices) and the area of low- and high-frequency electromagnetics.

Dr. Ghione is member of AEI (Associazione Elettrotecnica Italiana).

✠

Carlo U. Naldi (M'73) was born in Torino in 1939. He graduated in electronic engineering from the Politecnico di Torino, Torino, Italy, in 1967. Since then, he has been doing research there on microwave device modeling and design in the Department of Electronics.

In 1969, he became Assistant Professor of Applied Electronics and then of Microwave Techniques. Since 1970 he has also been Professor in charge of Solid State Electronic Devices; in 1982 he became Associate Professor and in 1986 Full Professor. Since 1977, he has been working on various ESTEC (European Space Agency) projects, mainly on quick steady-state algorithms for nonlinear circuit analysis, modeling and performance simulation techniques of GaAs MESFET's for microwave power amplifiers, and automatic design of MESFET amplifiers replacing TWTA. Since 1984 he has been involved in the European ESPRIT project in the field of MMIC's. His main research interests are now in the area of microwave linear and nonlinear circuit analysis and development and the modeling of passive and active components for MIC applications.

Dr. Naldi is member of the American Physical Society and of the UMI (Italian Mathematical Association).

✠

Fabio Filicori was born in Italy in 1949. He received a degree in electronic engineering from the University of Bologna, Bologna, Italy, in June 1974.

Since then he has been with the Faculty of Engineering of the University of Bologna, first as an Assistant Professor of Applied Engineering and then, beginning in 1982, as a Professor of Radio Electronics, teaching courses on computer-aided circuit design and power electronics. His current research interests are in the fields of nonlinear circuit analysis and design, electronic device modeling, and power electronics.